JOURNAL OF BACTERIOLOGY, Apr. 1992, p. 2160–2171
0021-9193/92/072160-12$02.00/0

Vol. 174, No. 7

Genetic Analysis of the Tn*21* *mer* Operator-Promoter

SOON-JUNG PARK,† JOY WIREMAN, AND ANNE O. SUMMERS*

Department of Microbiology, The University of Georgia, Athens, Georgia 30602

Received 1 August 1991/Accepted 27 January 1992

The mercury resistance operon, *mer*, of the transposon Tn*21* is transcribed from two overlapping divergent promoters: P_R for the regulatory gene, merR, and P_{TPCAD} for the structural genes, *merTPCAD*. Transcription of *merTPCAD* is repressed in the absence of Hg(II) and activated in the presence of Hg(II) by the regulatory protein, MerR. In addition, MerR represses its own expression regardless of the presence of Hg(II). MerR binds as a dimer to a single region of dyad symmetry lying between the −35 and −10 hexamers of P_{TPCAD}. Analysis of the expression of transcriptional fusions to hydroxylamine- and oligonucleotide-generated mutants of this divergent operator-promoter region identified key bases involved in MerR-dependent repression of P_{TPCAD} and of P_R and in activation of P_{TPCAD}. Six of the seven mutants affecting the palindromic region were altered in their ability to bind the MerR protein in vitro as measured by fragment retardation assays. These differences in in vitro MerR binding correlated well with the in vivo measurements of repression or of activation. Bases identified as functionally relevant by this genetic analysis coincide extensively with those previously identified as relevant via in vivo footprinting. Four major points emerge from this analysis: (i) transition and transversion mutations within the spacer between the −10 and −35 hexamers of P_{TPCAD} generally have little effect on the MerR-independent (i.e., unregulated) expression of either promoter; (ii) alteration of certain bases in the MerR-binding dyad affects repression of P_{TPCAD} differently than repression of P_R; (iii) certain dyad changes can impair activation of P_{TPCAD} more severely than repression of this promoter; and (iv) mutations in the −10 hexamer of P_{TPCAD} which also effect P_R expression define one of two potential −10 hexamers in P_R as actually functional in vivo.

Our current theory of how proteins recognize DNA sequences owes much to studies of bacteriophages lambda (39) and P22 (43) and to studies of catabolic (20, 36), biosynthetic (56), and resistance (3, 21) operons in *Escherichia coli* and *Salmonella typhimurium*. In many systems symmetrical elements in the regulatory protein and its cognate DNA binding site play a role in interaction (14). Such symmetrical protein and DNA elements are also implicated in the control of the bacterial mercury resistance (*mer*) locus, a surprisingly complex detoxification operon with several regulatory features not found in the above systems.

In the bacterial mercury [Hg(II)] resistance (*mer*) operon of Tn*21*, there are two tightly overlapped, divergently oriented promoters: P_R for the regulatory protein, *merR*, and P_{TPCAD} for the structural gene transcript, *merTPCAD*, which encodes a transport system (*merTPC*), mercuric reductase (*merA*), and *merD*, which may switch off expression when Hg(II) has been reduced to Hg(0) by MerA (Fig. 1) (8, 33, 57). The expression of P_{TPCAD} is repressed in the absence of Hg(II) and activated in the presence of Hg(II) by the *merR* gene product, and, despite its close overlapping with P_{TPCAD}, the expression of P_R does not change in the presence of Hg(II) (27, 34, 44). In vivo the initiation points of the *merR* and structural gene transcripts are separated by 17 bp (19, 26, 27). P_{TPCAD} has good correspondence to the consensus recognition sites for σ^{70} RNA polymerase (13, 15, 32) in its −10 and −35 hexamers, but it has a nonoptimal spacer of 19 bp (Fig. 2, darker-shaded boxes). The P_R promoter has two sets of potential RNA polymerase recognition sites, both of which correspond well to their respective consensus sequences but one of which (Fig. 2, vertically striped boxes) would have a 19-bp (nonoptimal) spacer and an 11-bp (nonoptimal) distance from the 3′ end of the −10 hexamer to the transcript start. The other set of potential RNA polymerase recognition sites for P_R (Fig. 2, lighter-shaded boxes) would have a 15-bp (nonoptimal) spacer and a 6-bp (optimal) distance from the 3′ end of the −10 hexamer to the transcript start.

The 144-amino-acid regulatory protein MerR binds as a dimer to a region of interrupted dyad symmetry (18 bp) located between the −35 and −10 hexamers of P_{TPCAD} (18, 19, 26, 37, 38). MerR is unique among activator proteins in binding between the two key recognition elements of sigma-70 RNA polymerase. When present, MerR always binds to *merOP*, and, surprisingly, when bound it fosters the occupancy of P_{TPCAD} by RNA polymerase regardless of whether Hg(II) is present, although MerR prevents the formation of an open complex by RNA polymerase until Hg(II) is added (9, 19). MerR also represses its own expression independently of Hg(II) (34). Genetic and biochemical analyses of *merR* mutants (16, 46, 54, 53) have identified a highly conserved helix-turn-helix motif in the amino terminus of MerR as the DNA binding domain and cysteine residues at positions 82, 117, and 126 as ligands in Hg(II) binding. MerR is capable of dimerizing in the absence of either DNA or Hg(II) in a manner which is not dependent on the formation of a disulfide bridge (53, 55). Genetic (16, 46, 53) and biochemical (37, 55, 62) evidence indicates that MerR binds Hg(II) with a very high affinity at one atom per dimer by using an unusual trigonal sulfur complex in which two cysteine-sulfur ligands are contributed by one monomer and the third cysteine-sulfur ligand is contributed by the other monomer. Thus, the Hg(II)-activated form of the MerR homodimer is an asymmetric structure.

In the work reported here we fused Tn*21* P_R to *phoA* and P_{TPCAD} to *lacZ* and used these constructs and another which was devised previously (46) to isolate mutants with loss or

* Corresponding author.
† Present address: Department of Microbiology, University of California—Los Angeles, Los Angeles, CA 90024.

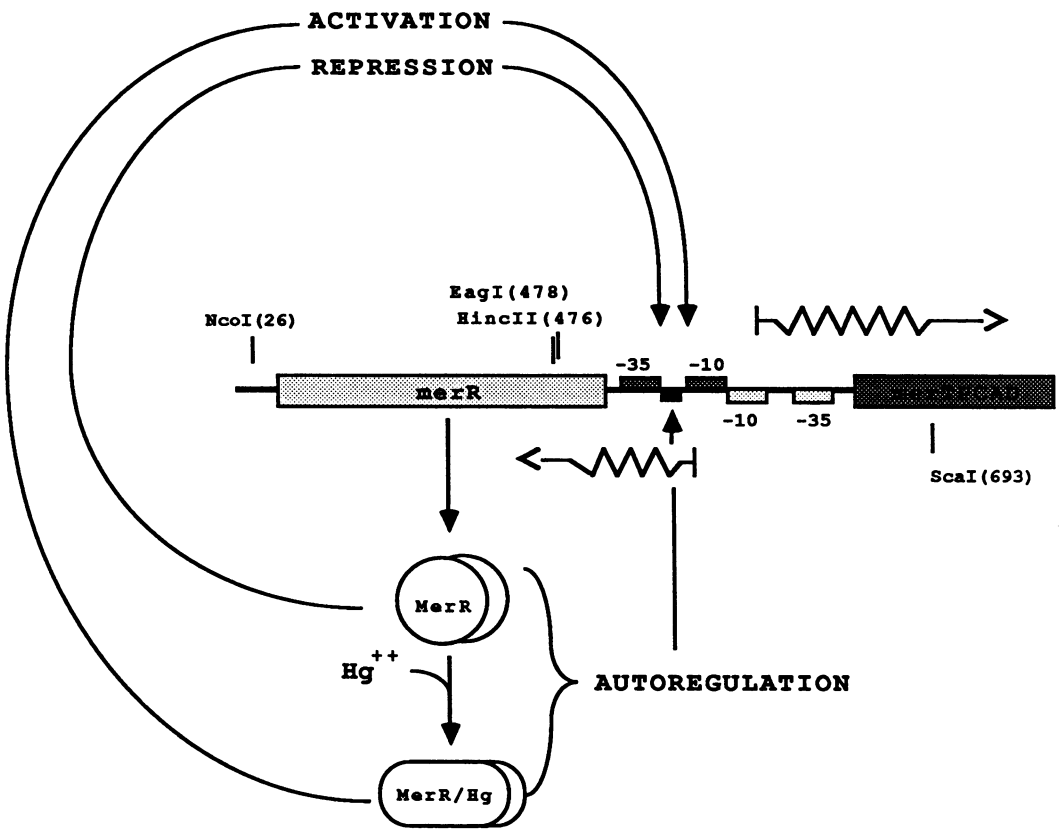

FIG. 1. Regulation of the *mer* operon of Tn*21*. Wiggly arrows indicate the direction of transcription of *merR* (lighter-shaded box) or of the structural genes *merTPCAD* (darker-shaded box). The corresponding −10 and −35 regions of the respective divergent promoters are indicated with the same shading. The solid box is the dyad symmetry region to which MerR binds. MerR is believed to undergo a conformational change upon addition of Hg(II), as indicated by the circle and lozenge shapes. Restriction sites and their corresponding nucleotide numbers (5) were converted to *Hin*dIII (*Nco*I or *Hin*cII) and *Bam*HI (*Sca*I) in pWR2 (44) and in pSJ51, respectively, to facilitate subcloning into reporter gene fusion vehicles (details in Materials and Methods).

gain of function in *merOP*. We characterized the mutants obtained with respect to the three in vivo activities of *merOP* (*merR* repression, *merTPCAD* repression, and Hg-dependent *merTPCAD* activation) and with respect to their ability to bind MerR protein in vitro in the presence and absence of Hg(II). We find that a given mutation can have distinct effects on these MerR functions and that the bases which are important in these functions correspond extensively, but not entirely, to those identified as important by in vivo (19) and in vitro (9, 37, 38) DNA footprinting.

(This work was submitted by S.-J. Park in partial fulfillment of the requirements for an M.S. from the University of Georgia.)

MATERIALS AND METHODS

Bacterial strains and plasmids. All plasmids used or constructed and the host strains used in this work are listed in Table 1.

Plasmid constructions (Fig. 1 and Table 1). An 8-bp unphosphorylated *Hin*dIII linker (no. 1002; New England Biolabs) was inserted either into the *Eco*RI site (at nucleotide [nt] 26; a linker replacing the natural *Nco*I site of Tn*21*) or into the *Hin*cII site (nt 476) of pWR2 (46) by the method of Lathe et al. (25). The resultant plasmids were named pSJ51 and pSJ53, respectively. There is also a *Bam*HI site in pWR2 which arose from a linker inserted into the natural *Sca*I site (nt 693) of Tn*21* (46). The 676-bp *Hin*dIII-*Bam*HI fragment from pSJ51 contains the *merR* gene, the entire *merOP* region, and 84 nt of *merT*. The 218-bp *Hin*dIII-*Bam*HI fragment of pSJ53, containing the first 57 nt of the *merR* coding region (called *merRΔ10*), the entire *merOP* region, and 84 nt of *merT* was subcloned into pCB267, a bidirectional promoter cloning vehicle (Table 1) (51), to give plasmid pSJ43 which contains *merRΔ10-phoA* and *merT'-lacZ* transcriptional fusions (Table 1).

β-Galactosidase assay. Overnight cultures in Luria broth with 50 μg of ampicillin per ml and 25 μg of kanamycin per ml were diluted 1/20 with fresh Luria broth. The cells were grown to ~25 Klett units and aliquoted into separate flasks for Hg(II) induction. Aliquots were incubated either with Hg(II) (2 μM) or without Hg(II) for an additional 20 min at 37°C. The cultures then were chilled rapidly on ice to prevent further induction and/or growth and then washed with minimal medium basal salts (30) including antibiotics but no carbon source or amino acids and were assayed for β-galactosidase (30).

Alkaline phosphatase assay. Cells were prepared as for the LacZ assay except that after the induction period, they were washed with Tris medium (51) containing antibiotics but lacking a carbon source and amino acids. The washed cells were suspended in 1 ml of 1 mM Tris-HCl (pH 8.0). After lysis of the cells with 40 μl of chloroform per ml and 0.002%

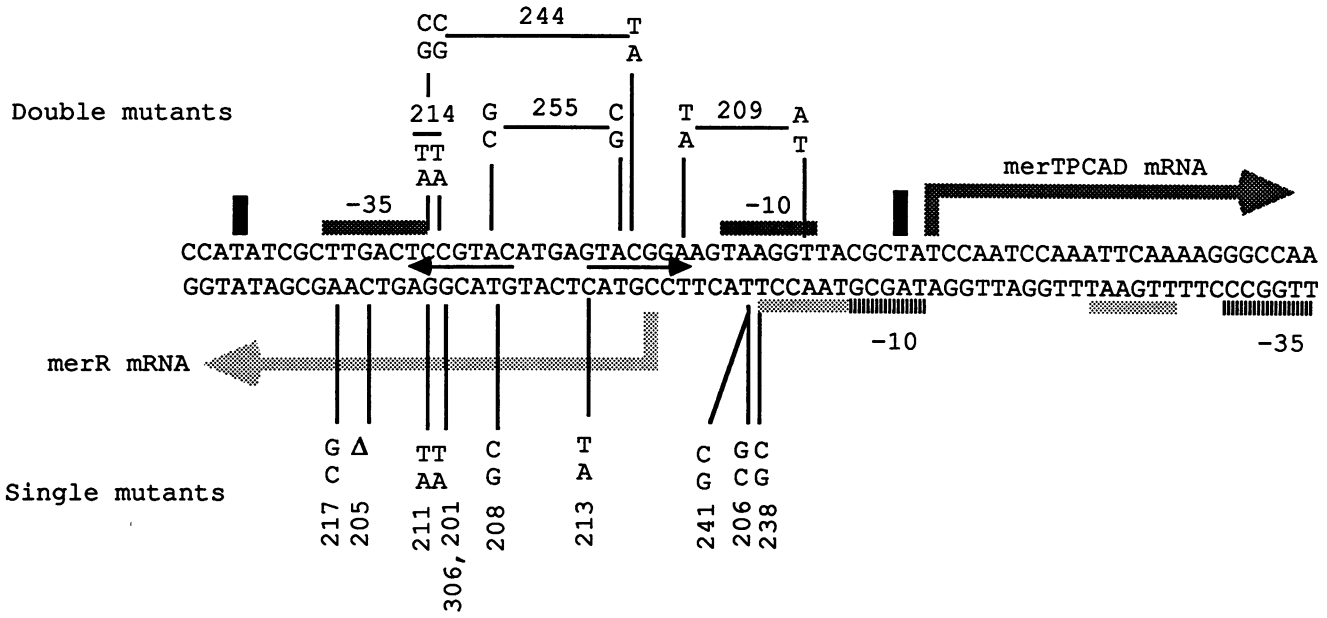

FIG. 2. Sequence alterations in *cis*-acting mutants of Tn*21 merOP*. Single mutants are indicated below the wild-type sequence, and double mutants are indicated above the wild-type sequence. Note that mutant 244 has an insertion after position −32 and a transversion at position −19. The solid arrows between the strands indicate the palindromic MerR binding region. The −10 and −35 hexamers of the structural gene transcript (top strand) and the *merR* transcript (bottom strand) are indicated by bars whose shading corresponds to the relevant transcript (indicated by large shaded arrows). There is an additional possible set of −10 and −35 hexamers in P_R, indicated by the vertically striped boxes (see the introduction). The extent of the oligonucleotides used for mutagenesis is indicated by the single vertical black bars at positions −2 and −44 of P_{TPCAD}. The outermost 6 nt at each end of these 43-nt oligomers were synthesized with the wild-type sequence. The inner 31 bp (extending from the entire −35 hexamer through the entire −10 hexamer of P_{TPCAD}) were synthesized with a 3% chance at each position of inserting an incorrect nucleotide.

sodium dodecyl sulfate, the reactions were started by addition of 100 μl of 4% 4-nitrophenylphosphate solution and the reaction mixtures were incubated at 37°C. To stop the reactions, 100 μl of KH_2PO_4 (1 M, pH 8.0) was added, and the cell debris was removed by centrifugation. Alkaline phosphatase activity was determined as described by Schneider and Beck (51).

Hydroxylamine mutagenesis. Plasmid pWR2 DNA containing the *merT'-lacZ* fusion was treated with hydroxylamine as described by Ross et al. (46) and transformed into CAG1574, a *recA lacZ* strain. Transformants were plated on 5-bromo-4-chloro-3-indolyl-β-D-galactopyranoside (X-Gal) indicator plates without Hg(II). Three isolates (pWR201, pWR211, and pWR214) with increased expression of β-galactosidase were characterized further.

Oligonucleotide-directed mutagenesis of P_{TPCAD}. Forty-three-base oligomers corresponding to the bottom-strand region of P_{TPCAD} containing the −10 hexamer, the −35 hexamer, and spacer region including the MerR binding site (region between vertical black bars in Fig. 2) were synthesized. The outer 6 bases on each end were synthesized as the wild-type sequences, and the inner 31 bases of the oligomers were synthesized with 3% incorrect dNTPs (1% each). The ratio of incorrect dNTPs to correct dNTPs was calculated to

TABLE 1. Bacterial strains and plasmids

Strain or plasmid	Genotype or phenotype	Source
Strains		
Escherichia coli K-12		
CAG1574	*araD139* Δ(*ara leu*)*7697* Δ*lacX74 galU galK hsdR rpsL recA56 srl*	W. Ross
CB806	Δ*lacZ lacY*$^+$ *galK phoA8 rpsL thi recA56*	C. Beck
Plasmids		
pCB267	*lacZ*$^+$ *phoA*$^+$; Amp^r pBR322 replicon	C. Beck
pNH9	*merR*$^+$ *merOP*$^+$; Kan^r p15A replicon	N. Hamlett
pACYC177 AmpΔ	Kan^r p15A replicon	W. Ross
pSJ43	*phoA-R*(Δ*10*)*-T'-lacZ*; Amp^r pBR322 replicon	This study
pSJ51	*merR*$^+$ *merOP*$^+$ *merT'-lacZ*$^+$; Amp^r pBR322 replicon; *Hin*dIII linker replaces *Eco*RI at nt 26 of pWR2	This study
pSJ53	as for pSJ51 but with *Hin*dIII linker replacing *Sca*I-*Bam*HI site at nt 476	This study
pWR2	*merR*$^+$ *merOP*$^+$ *merT'-lacZ*$^+$; Amp^r pBR322 replicon; *Eco*RI site replaces *Nco*I site at nt 26 of natural *mer* operon	W. Ross

yield single point mutations rather than double or triple mutations (6). The oligomers were inserted into either pSJ51 (*merR-merOP-merT'-lacZ* transcriptional fusions) or into pSJ43 (*merRΔ10'-phoA* and *merT'-lacZ* transcriptional fusions) by the method of Inouye and Inouye (22) as follows. Plasmids pSJ51 and pSJ43 were digested with *Pst*I and treated with alkaline phosphatase, resulting in a single cut in the *bla* gene. Separate aliquots were treated with *Bam*HI or *Hin*dIII, and the larger fragment lacking the *mer* sequence was separated by electrophoresis and recovered by electroelution. The oligomer was diluted with 0.1× Tris-EDTA buffer to a concentration of 20 pmol/μl, and its ends were phosphorylated with T4 polynucleotide kinase. The *Pst*I-digested DNA, the *Bam*HI-*Hin*dIII larger fragment (0.3 μg each), and phosphorylated oligomer (75 pmol) were mixed and incubated at 100°C for 3 min. A series of incubations at 30 and 4°C and on ice resulted in renaturation of DNA. The gaps in the renatured DNA were filled in with Klenow polymerase and the DNA was ligated overnight at 15°C.

Screening and selection of mutants. Mutagenized pWR2 or pSJ51 DNA was transformed into CAG1574 (for pSJ51 or pWR2) or CB806(pNH9) (for pSJ43), and the cells were plated on media containing X-Gal and 2 μM Hg(II), a concentration of Hg(II) which readily induces the *mer* operon but which is in itself not toxic for cells lacking the functional mercury detoxification system provided by the intact *mer* operon. However, on plates containing inducing concentrations (2 μM) of $HgCl_2$, strains carrying pSJ51 or pWR2 which have the wild-type *mer* regulatory elements fused to *lacZ* do not form colonies but produce a dark blue stain in the agar ("blue ghosts"), apparently the result of excessive production of the toxic X-Gal hydrolysis product leading to cell lysis (reference 46 and our unpublished observations). Thus, this strategy was useful for recovering mutants whose Hg(II)-induced expression is less than that of the wild type. Since strains carrying wild-type pWR2 or pSJ51 become pale blue on X-Gal medium lacking Hg(II) in less than 16 h, these constructs were less useful for screening for variants with increased operon expression. Another construct, pSJ43, the *merT'-lacZ* and *merR'-phoA* transcriptional fusion (to which *merR* is supplied in *trans* by pNH9), has a very low background level of *lacZ* expression (it remains white on X-Gal plates for at least 48 h), and growth on X-Gal of strains containing pSJ43 and pNH9 is not impaired by induction with 2 μM Hg(II). Thus, Amp^r Kan^r transformants containing mutagenized pSJ43 and wild-type pNH9 were screened for increased operon expression on X-Gal indicator plates without Hg(II).

Phenotype determination. Transformants arising after mutagenesis were compared on X-Gal indicator plates [with or without 2 μM Hg(II)] with strains carrying the wild-type parental plasmid. Stable isolates were divided into the following three groups: group I, those which, in the absence of Hg(II), had less expression than the parent; group II, those whose uninduced expression was equivalent to that of the parent; and group III, those which had more expression than the parent. Plasmid DNA of representatives of each group was transformed into CAG1574 to confirm the association of the mutant phenotype with the plasmid and into CAG1574(pNH9) to discover whether the mutation was *cis* dominant. The *Eag*I-*Bam*HI restriction fragment (nt 478 to 693 [linker] containing the *merR'-merOP-merT'* genes) of each promising mutant was used to replace the corresponding fragment of the unmutagenized parental plasmid. For each mutant found by marker replacement to lie within the *merOP* region, a *merR* deletion derivative was made by removing DNA between *Hin*dIII (nt 26 [linker]) and *Eag*I (nt 478) in order to measure the *merR*-independent expression of P_{TPCAD}. The effect of each mutation on *merR* expression was determined by exchanging the *Eag*I-*Bam*HI fragment of each mutant with the corresponding fragment of pSJ43 which has a *merR'-phoA* transcriptional fusion. Repressed and derepressed levels of P_R were determined by assaying alkaline phosphatase activities of strains containing mutant pSJ43 with either pNH9 or pACYC177 Amp^{Δ}, respectively, in *trans*.

DNA sequence analysis. For those pSJ51 derivatives whose defect lay in the *Eag*I-*Bam*HI fragment (nt 478 to 693 [linker]), the appropriate restriction fragment was subcloned into M13mp18 and M13mp19 (63) and sequenced on both strands (47) by using a specific *merR* primer and the M13 sequencing primer. For mutants obtained in pSJ43, the *Hin*dIII-*Bam*HI fragment (nt 472 [linker] to nt 693 [linker]) was used for sequence determination with M13 as above.

Fragment retardation assay. Cell lysates either containing MerR or lacking it were prepared by using the T7 overexpression system as implemented by Heltzel et al. (18). CsCl-purified DNA (0.7 μg) of wild-type or mutant plasmids was digested with *Eag*I and *Bam*HI and labeled with 6 μCi of [α-^{32}P]dGTP by using DNA polymerase I (Klenow fragment). The smaller fragment (218 bp) of the two fragments resulting from the double digestion contained the *merOP* region. MerR-DNA complexes were formed in a 10-μl solution containing 10 mM Tris-HCl (pH 7.4), 1 mM EDTA, 50 mM KCl, 0.1 mM dithiothreitol, 0.5 μg of herring sperm DNA (10), ~2 ng of labeled DNA, and MerR lysates in various amounts from 0.005 to 4 μg of protein. After DNA and protein lysate were combined in the reaction buffer, the combination was mixed gently and incubated at room temperature for 15 min. One microliter of stop dye (50% glycerol, 0.1% bromophenol blue) was added, and the reaction was loaded onto a 12% polyacrylamide gel (acrylamide/bis, 29.2:0.8 [wt/wt] in Tris-borate-EDTA) whose wells were preloaded with 40 μl of binding buffer containing 100 mM KCl. For assays in the presence of Hg(II), cell protein lysates were preincubated with 1 μM $HgCl_2$ (a concentration known to be effective for induction in vitro [9, 16, 37, 38] and in vivo [19]) for 15 min before being combined with DNA and EDTA was omitted from all reaction buffers. After 3.5 h of electrophoresis at room temperature, the gels were dried on Whatman filter paper at 60°C under vacuum and exposed to X-Omat AR film (Kodak) at −70°C for 4 to 12 h; two or more exposures were made for each gel to optimize exposures for densitometry (10). For each lane, the ratio of the MerR-DNA complex to the sum of the free DNA and the MerR-DNA complex (percent bound) was determined densitometrically (scanning laser densitometer; Biomed Instruments, Inc., Fullerton, Calif.). The percent of fragment bound was plotted as a function of the amount of protein lysate added to the reaction buffer, and for each mutant the amount of protein necessary to retard 50% of the labelled *merOP* DNA fragment was determined graphically. Results of assays with the mutant *merOP* DNAs, obtained by using two independently prepared MerR protein lysate preparations, were equivalent.

RESULTS

Mutagenesis of *merOP*. Random mutagenesis of the *mer-lac* fusion plasmid pWR2 with hydroxylamine was previously found to be effective for isolation of mutations in the structural gene of the *mer* regulatory protein MerR (46). However, many of the *cis*-acting hydroxylamine mutants of

pWR2 simply had alterations in the plasmid copy number as detected by gel electrophoresis. Of those "up-expression" mutants not resulting from copy number changes, three (mutants 201, 211, and 214) proved to lie in the *merOP* region and were examined in detail in this study (each number refers to a distinct mutant plasmid; for simplicity's sake the mutants are designated simply by their numbers in the text rather than by the longer "pSJ---" or "pWR--" format used for the parental plasmids). The paucity of *merOP* mutants arising from hydroxylamine mutagenesis led us to employ oligonucleotide-directed mutagenesis of the palindromic region and the immediately adjacent −10 and −35 hexamers of the structural gene promoter, P_{TPCAD}. By using a mutagenic oligonucleotide, we obtained 69 "down-expression" mutants from pSJ51 (P_{TPCAD}-*lacZ*) by virtue of their ability to grow on X-Gal plates with 2 μM Hg(II). These isolates were divided into three groups on the basis of their behavior on X-Gal media lacking Hg(II): group I, those with less expression than the parent; group II, those with expression equivalent to that of the parent; and group III, those with more expression than the parent. After variants with copy number changes were eliminated and the *cis* dominance of the remaining variants was confirmed, typical representatives of each group were chosen for more detailed examination (group I, 101, 205, 209, 241, and 219; group II, 170, 213, 206, and 217; and group III, 208, 231, 238, 242, 244, and 255). The three hydroxylamine mutants noted above fell into group II (211 and 214) and group III (201) in this classification.

Plasmid pSJ51 is sufficiently "leaky" in its expression that it is relatively difficult to discern colonies with increased blueness on medium lacking Hg(II). Thus, pSJ43, which remains white on X-Gal plates for more than 48 h (with *merR* in *trans*), was used to screen on Hg-free medium for other up-expression mutants. Of 28 blue isolates (among ca. 600 transformants derived from oligonucleotide mutagenesis of pSJ43), the majority were found to have increased copy number. Upon retransformation and marker replacement of those with unaltered copy number, only one of these (306) was found to lie in the *merOP* region; its properties placed it in group III.

Location of the mutant lesions in *merOP*. Each mutant whose location in *merOP* was confirmed by marker replacement and *cis* dominance was subjected to DNA sequence analysis (Fig. 2) prior to more extensive physiological and physical analyses. The majority of the mutants had single lesions. With the exception of the four double mutants noted below, all mutants with more than one lesion were eliminated from the study. Group I mutants had occurred in the −35 (205) or the −10 (241) RNA polymerase recognition elements of P_{TPCAD} or in the −10 hexamer and the right dyad arm (double mutant 209). Mutant 205 has a deletion of the G at position −36, a key RNA polymerase recognition element in the *mer* system (19, 37). Two group I mutants (101 and 219) had no detectable changes in the *merOP* region or in the ca. 50 flanking bp on either side and were not examined further. Group II mutants had occurred in the −10 and −35 hexamers (206 and 217, respectively) and in the left (211 and 214 [double]) and right (213) dyad arms. Group II mutant 170 had multiple changes immediately adjacent to the oligonucleotide target site and was not examined further. Group III mutants had occurred in the dyad arms (201, 208, and 244 [double]; 255 [double]; and 306) and in the −10 hexamer (238). Note that two independent mutagenesis and screening strategies resulted in the same change CG→TA at position −31 in the left dyad arm (201 and 306). Group III mutants 231 and 242 had no detectable changes in the *merOP* region and were not studied further.

Determination of phenotypes of *cis*-acting mutants. The unregulated activity for P_{TPCAD} and for P_R (i.e., the *merRΔ10* condition) of each mutant was compared with that of the respective parental plasmid (Tables 2 and 3). We found that some mutants differed only slightly (e.g., 208, 211, and 255) and others differed markedly (e.g., 201, 205, and 238) from their parents. Therefore, because changes in regulated expression (i.e., the $merR^+$ condition) may be influenced by underlying changes in the ability of the promoter to function by itself (i.e., with RNA polymerase alone), we used each mutant's unregulated activity as the reference point in comparing its ability to be repressed or activated by MerR (Tables 2 and 3) with that of the unmutagenized parent.

(i) Effects on the unregulated expression of P_{TPCAD} (Table 2) and of P_R (Table 3). Since the P_{TPCAD} and P_R promoters overlap to some degree, a given mutation could affect the unregulated expression of both promoters. We were interested in whether the effect of a given mutation was the same or different for the two promoters. As expected, mutations lowering the unregulated expression of P_{TPCAD} lay in the −35 or −10 hexamers of this promoter (single mutants 217, 205, 206, 241, and 238 and double mutant 209) (Table 2). Three of these mutations (206, 241, and 238) also lowered unregulated expression of P_R (Table 3); all three change TA or AT pairs to CG or GC pairs and would make the −10 region of P_R more difficult to melt (Fig. 2). Mutant 238 alters a highly conserved (32) position in one of the two putative −10 hexamers of P_R. The strong effect of mutant 238 on P_R function suggests that it is the −10 hexamer nearer to the start position of *merR* mRNA that is actually used (Fig. 2, lighter-shaded box). Two of the mutants in the RNA polymerase recognition hexamers of P_{TPCAD}, single mutant 217 (in which G replaces T at position −38 [T-38G]) and double mutant 209 (A-16T, T-8A), increase unregulated P_R expression (Table 3). Mutant 209 brings the start-site-proximal −10 of P_R closer to consensus while taking P_{TPCAD} further from consensus (32). Alterations in the spacer region between the −10 and −35 hexamers of P_{TPCAD} (i.e., in the MerR-binding dyad) do not significantly affect the intrinsic promoter strength of either of the divergently transcribed promoters.

(ii) Effects on repression of P_{TPCAD} (Table 2) and P_R (Table 3). Since the mutants differ in their unregulated promoter strengths, to evaluate the repressibility of the mutant *merOP*s we compared each mutant's unregulated expression to its repressed expression (Tables 2 and 3). The expression of P_{TPCAD} was examined with *merR* in *cis*, as it occurs naturally (i.e., in pSJ51 derivatives). However, as *merR* is deleted in forming the P_R-*phoA* reporter fusion (pSJ43), it was necessary to assess P_R function with *merR* in *trans* (on pNH9). Since the behavior of P_{TPCAD} with *merR* in *trans* correlates well with that of *merR* in *cis* for wild-type pSJ43 and for most of the mutant derivatives (data not shown; note that absolute expression of P_{TPCAD} in pSJ43 is considerably lower than in pSJ51), we make the working assumption here that *merR-phoA* expression in pSJ43 and its mutant derivatives accurately reflects the natural expression of P_R.

As both promoters are repressed by MerR, we can ask whether a given mutation affects P_R repression differently than P_{TPCAD} repression. Mutants in the interhexamer region (211, 201, 214, 208, 255, 213, and 244) have robust intrinsic promoter activities, and thus clearer distinctions can be made among them with respect to their ability to repress the two promoters. The three spacer region mutants which are

TABLE 2. Expression of *merOP-merT'-lacZ* fusions

Allele	Change	MerR	LacZ activity[a]		Relative unregulated activity	Relative repression[b]	Relative activation[c]
			Without Hg(II)	With Hg(II)			
Wild type[d]		−	2,435	2,296		3.7	8.6
		+	657	19,837			
217	T-38G	−	292	275	0.1	2.0	15.1
		+	146	4,156			
205	G-36Δ	−	681	643	0.3	5.6	0.14
		+	122	92			
211	C-32T	−	2,605	2,732	1.1	2.4	4.9
		+	1,096	13,293			
201	C-31T	−	10,568	10,286	4.4	4.1	2.5
		+	2,557	25,279			
214	CC-32,-31TT	−	3,263	3,742	1.3	2.6	3.1
		+	1,266	11,595			
208	A-28C	−	2,143	2,158	0.9	1.4	1.3
		+	1,534	2,732			
255	A-28G, A-20C	−	3,628	3,171	1.5	1.2	2.7
		+	2,971	8,518			
213	G-22T	−	3,117	3,168	1.3	7.1	0.9
		+	438	3,008			
244	C-19T, C-32CC	−	3,750	3,995	1.5	4.2	0.3
		+	901	1,125			
209	A-16T, T-8A	−	122	138	0.05	0.7	17.8
		+	170	2,457			
241	A-12C	−	317	295	0.1	13.0	0.2
		+	24	69			
206	A-12G	−	219	184	0.1	3.0	0.7
		+	73	138			
238	A-11C	−	388	392	0.2	0.5	18.9
		+	730	7,370			

[a] Average standard deviations are ca. 10% for values > 100 units and ca. 20% for values < 100 units.
[b] Relative repression = derepressed activity (without MerR)/repressed activity (with MerR).
[c] Relative activation = activated activity (with MerR, with Hg^{2+})/derepressed activity (with MerR).
[d] Wild type is pSJ51, *merOP-merT-lacZ* fusion.

affected only slightly in repression of both P_{TPCAD} and of P_R (single mutants 211 and 201 and double mutant 214) alter outer bases of the left dyad arm. In fact, single mutant 211 and double mutant 214 both affect C-32, which is the overlap position shared by the −35 hexamer and the left dyad arm. Three of the spacer region mutants which markedly impair repression of one or both promoters affect inner bases in both dyad arms (single mutant 208 and double mutants 255, and 244). Both changes in 255 affect inner bases in the left and right dyad arms; the changes in 244 affect an inner position in the right dyad arm (C-19T) and engender an insertion at an outer position in the left dyad arm (C-32CC). The insertion of a T at this same left-arm position in Tn*501* (this would be the equivalent of C-32CT in Tn*21*; Fig. 2) did result in a loss of repressibility (the +1 mutation reported in reference 42); the effect of the +1 mutation on P_R expression in Tn*501* was not assessed (42).

The behavior of mutant 213 (G-22T) is especially interesting. This transversion mutant at the innermost position of the right dyad arm represses P_{TPCAD} quite well and P_R somewhat less well, although it is clearly more effective in P_R repression than its immediate neighbors, 208, 255, and 244. Similarly, in the Tn*501 merOP* a transversion mutation (C565A) at the symmetrical position in the left dyad arm (which would be position −27 in Fig. 2) repressed the Tn*501* P_{TPAD} promoter as effectively as the wild type; the effect of C565A on Tn*501* on P_R expression was not assessed (42). Mutant 213's competence in repression contrasts strongly with its impairment in activation of P_{TPCAD} (see below), as did that of the symmetrical mutant C565A in Tn*501* (42).

Mutants in the −10 and −35 regions of P_{TPCAD} (217, 205, 209, 241, 206, and 238) are sufficiently impaired in either one or both of their intrinsic promoter activities to limit conclusions about their differential effects on repression of the two promoters. Nonetheless, it is important that double mutant 209, which has strong intrinsic P_R expression, is very effective in repressing P_R, suggesting that it is able to bind MerR (see below).

(iii) Effects on activation of P_{TPCAD} (Table 2). Since activation of P_{TPCAD} could be influenced by the underlying strength of the unregulated promoter, each mutant's activated expression is considered with respect to its unregulated expression (relative activation) as well as with respect to its absolute induced activity compared with that of the wild type (Table 2). Three mutants in the left arm of the dyad (201, 211, and 214) can still be activated (Table 2), suggesting that they are able to bind MerR (see below and Table 5).

The dyad mutants most profoundly impaired in activation have one or more lesions in the inner bases of each dyad arm (208, 255, 213, and 244). Double mutant 255 is capable of only modest inducibility beyond its intrinsic expression level, and 208, 213, and 244 are simply not activatable (although, as noted above, their intrinsic expression is not materially different from that of the wild type). It appears that changes in positions in the dyad arms which are closer to the center of the dyad (i.e., the inner positions) have

TABLE 3. Expression of *merOP-merR'-phoA* fusions

Allele	Change	MerR[a]	PhoA activity[b]		Relative unregulated activity	Relative repression[c]
			Without Hg	With Hg		
Wild type[d]		−	1,547	1,436		50.0
		+	31	29		
217	T-38G	−	2,970	2,743	1.9	29.6
		+	93	100		
205	G-36Δ	−	1,346	1,264	0.9	17.5
		+	77	72		
211	C-32T	−	2,181	2,527	1.4	32.3
		+	62	86		
201	C-31T	−	1,825	1,996	1.2	52.7
		+	31	43		
214	CC-32, -31TT	−	1,952	2,283	1.3	20.4
		+	94	115		
208	A-28C[e]	−	2,166	2,326	1.4	2.9
		+	743	833		
255	A-28G, A-20C	−	1,948	2,109	1.3	1.3
		+	1,563	1,680		
213	G-22T	−	3,110	3,475	2.1	9.8
		+	325	345		
244	C-19T, C-32CC	−	3,017	3,174	2.0	1.4
		+	1,951	2,111		
209	A-16T, T-8A	−	5,198	4,796	3.3	83.8
		+	62	57		
241	A-12C	−	882	804	0.6	28.0
		+	31	29		
206	A-12G	−	650	646	0.4	22.0
		+	30	28		
238	A-11C	−	31	38	0.02	1.5
		+	16	29		

[a] *merR* provided in *trans* by pNH9.
[b] Average standard deviations are ca. 8% for values > 50 units and ca. 12% for values < 50 units.
[c] Relative repression = derepressed activity (without MerR)/repressed activity (with MerR).
[d] Wild type is pSJ43, *merR'-phoA* and *merT'-lacZ* fusions.

TABLE 4. In vitro binding of MerR to *merOP* DNA

Allele	Change	Lysate protein (μg) resulting in 50% binding[a]	
		Without Hg	With Hg
Wild type		0.18	0.22
217	T-38G	0.04	0.27
201	C-31T	0.21	0.30
209	A-16T, T-8A	0.13	0.28
211	C-32T	0.27	0.60
213	C-22T	0.60	0.40
214	C-31T, C-32T	0.43	0.70
208	A-28C	1.30	2.80
244	C-19T, C-32CC	1.60	4.00
255	A-28G, A-20C	>4.00	>4.00

[a] Percent of total labelled *merOP* fragment bound was determined densitometrically; see Materials and Methods.

greater influence on functions which require the binding of MerR (repression and activation) than do changes in the dyad positions which are farther from the center of the dyad (i.e., the outer positions on the arms).

Only three nondyad mutants (205, 206, and 241) are completely defective in P_{TPCAD} activation. The other three nondyad mutants (217, 238, and double mutant 209) can still be activated, although the absolute level of LacZ activity is still far less than in the parental strain (Table 2). Thus, within the −10 and −35 hexamers there are some changes from ideality that can be partially compensated for by MerR-mediated activation and others which cannot. Finally, expression of *merR* is known not to be influenced by Hg(II) (8, 34) and, while P_R-directed expression in several mutants increased slightly upon Hg(II) addition (Table 3), none is statistically different from the wild type in this respect.

Ability of *merOP* mutant DNA to bind MerR in vitro. Since the in vivo assays described above indicated that certain *merOP* bases play distinct roles in activation and repression, we used fragment retardation to assess the in vitro MerR binding ability of the *merOP* mutants. The effect of Hg(II) on MerR-DNA binding was also examined since there is evidence that, in vitro, the addition of Hg(II) can reduce the affinity of $MerR^+$ for $MerOP^+$ DNA (16, 17, 37, 39) or increase it (54). We examined the seven mutants lying within the known MerR binding region and the two mutants which are most distant from the MerR binding site and which lie in the RNA polymerase recognition sites for P_{TPCAD} at T-37 (217) and at T-8 (209). The latter mutant (209) is interesting in that it also has an alteration in the most 3′ base of the right dyad arm (A-16). Apparent binding constants derived from densitometry allowed us to group these mutants with respect to their affinity for MerR in vitro (Table 4). The first group (single mutants 217 and 201 and double mutant 209) bound MerR with an affinity equal to that of the wild-type *merOP* DNA. The second group (211, 213, and 214) is moderately impaired and requires from 1.5- to 3.3-fold more MerR to retard 50% of the fragment DNA. The third group is strongly impaired in binding and requires from 7- to 22-fold more MerR to retard 50% of the *merOP* DNA fragment. All but one of these *merOP* mutants are less able to bind to the MerR-Hg(II) complex than to MerR alone; only the moderately impaired mutant 213, like the wild-type *merOP*, binds well both to MerR and the MerR-Hg(II) complex.

Comparison of the in vitro MerR binding properties of the mutants with their in vivo repression and activation behavior reveals some expected correlations and some interesting contrasts (Table 5). Repression of P_R correlates well with the MerR binding ability of all mutants examined. Repression of P_{TPCAD} also correlates well with in vitro MerR binding ability, with two notable exceptions; single mutant 213 and double mutant 244 are unimpaired for repression of P_{TPCAD}, although they have moderate and severe defects, respectively, in both MerR binding and P_R repression. Finally, MerR binding of all mutants examined correlated well with the activatibility of P_{TPCAD}; thus, the inability of mutants 213 and 244 to activate P_{TPCAD} correlates well with their inability to bind MerR in vitro and less well with their proficiency in repressing P_{TPCAD} in vivo. It is also interesting that in mutant 209 the A→T change in the most 3′ position of the right dyad arm (A-16T) does not impair the in vitro MerR binding ability. Interestingly, both the Tn*501* and Tn*21* MerR proteins bound effectively in vitro to the *Bacillus merOP* DNA, which has a G at the same position (17, 55) (Fig. 3A). Thus, 209's deficit in expression of P_{TPCAD} (compared with the wild type) can be ascribed to its other defect, a nonconsensus change (32) in the most 3′ base of the −10 hexamer of P_{TPCAD}. Although this latter change gives mutant 209 a very poor intrinsic promoter, it does not completely prevent 209 from being activated by MerR, albeit to low absolute activity compared with the wild-type promoter.

TABLE 5. Comparison of MerR in vitro binding with repression and activation efficiencies of *merOP* mutants

Allele	Change	MerR binding defect	Repression defect[a]		Activation defect[a] (P_{TPCAD})
			P_R	P_{TPCAD}	
217	T-38G	None	None	—[b]	Moderate
201	C-31T	None	None	None	None
209	T-8A, A-16T	None	None	—	Moderate
211	C-32T	Moderate	Moderate	Moderate	Moderate
213	G-22T	Moderate	Moderate	None	Severe
214	C-31T, C-32T	Moderate	Moderate	Moderate	Severe
208	A-28C	Severe	Severe	Severe	Severe
244	C-19T, C-32CC	Severe	Severe	None	Severe
255	A-20C, A-28G	Severe	Severe	Severe	Severe

[a] Assignment to the three defect categories was on the basis of the repressibility or activatability (as defined in the footnotes to Tables 2 and 3) and also with respect to the absolute activity compared with that of the wild type.
[b] —, enzyme activities are too low to make precise distinctions.

DISCUSSION

Selection and screening for gain- or loss-of-function mutants has allowed us to identify key bases in the *merOP* of Tn*21*. We can consider these alterations in light of (i) the naturally occurring variations in the *OP* region of the *mer* operons of two gram-positive bacteria and four gram-negative bacterial plasmids (Fig. 3A) (2, 5, 12, 17, 24, 28, 31, 58a) and (ii) biochemical observations of the contacts made in Tn*21* and Tn*501* by MerR and RNA polymerase in repression and activation (9, 17, 38).

(i) Consideration of the mutants in light of the *merOP* consensus. The *merOP* region is very well conserved in gram-positive and in gram-negative genera, despite the fact that in the latter *merR* is not transcribed divergently but is the first gene in a transcript which includes all of the structural genes (16). In all cases studied the dyad symmetry region lies within the −35 to −10 spacer and is offset toward the −35 hexamer. Within the 18-bp *merOP* palindrome itself there are eight completely conserved bases (nnnGTACnn · nnGTACnnn). We found mutations in one out of four of these positions in the left dyad arm and in three out of four of these positions in the right dyad arm (Fig. 3A). The single mutation in the left arm GTAC (208) occurred in the only position (−28) in which no mutations were found in the corresponding position of the right dyad arm (−21). Similarly, the three mutations found in the right dyad arm GTAC (213, 244, and 255) occurred in positions in which no mutations were found in the corresponding positions of the left dyad arm. The next most conserved *merOP* bases are the three outlying bases in each dyad arm (TCCnnnnnn · nnnnnnGGA). These outer dyad bases are completely conserved in the four gram-negative operons but not in the gram-positive examples. We found mutations in the left arm CCs repeatedly (201, 211, 214, and 306) but none in the right arm GGs. Asymmetry in operator recognition in both prokaryotic and eukaryotic systems has been noted (4, 7, 35, 40, 41, 45, 48–52, 58–60), and since biochemical evidence shows that during induction the MerR homodimer binds a single atom of Hg(II) in an asymmetrical trigonal complex, it may be that MerR makes asymmetrical contacts with the operator dyad before and/or after induction.

The insertion in double mutant 244 replaces the 5′-most T of the left dyad arm with a C, which is the base occurring naturally at this position in the *Bacillus* and *Staphylococcus* operons. Two considerations suggest that this insertion may play a smaller role in the phenotype of 244. First, MerR of Tn*501* binds to the *Bacillus merOP* region with an affinity equivalent to that for the Tn*501 merOP* (17, 55), indicating that a T or C is acceptable at this position. Further, as noted above, in mutant 209 the 3′ end of the right dyad arm is changed (A-16T), but this does not affect MerR binding (Table 4), further suggesting that the outer bases of the dyad arms are less significant in MerR recognition. Thus the severity of mutant 244's MerR-binding-related behaviors likely arises from the loss of an important MerR contact at −19 in the right dyad arm (see also DNA footprinting considerations below) and, perhaps, from the insertion of an additional base between the RNA polymerase binding hexamer (−33 to −38) and the MerR binding site. The importance of close apposition of the left dyad arm and the −35 hexamer of P_{TPAD} has also been shown with Tn*501* (42).

The four-base central interruption between the conserved palindromic arms is less well conserved (Fig. 3A). There is a tendency for three of the four central bases (especially the leftmost two bases) to be A or T rather than G; C is not found at all (in the top strand). Both in vitro (9) and in vivo (19) DNA footprinting indicate MerR-dependent DNA distortions in this region which are concomitant with Hg(II) induction. Since no loss-of-function mutants were found in this region, the relevance of its specific sequence remains an unanswered question.

The −10 and −35 RNA polymerase recognition sites are highly conserved in the gram-negative operons and retain considerable homology to the eubacterial major sigma factor consensus even in the gram-positive versions of the *mer* operon. All of the P_{TPCAD} down-expression mutations isolated in these two regions (mutants 217, 205, 209, 241, 206, and 238) arose from changes which move key bases farther from consensus (13, 23, 29, 32). Of the mutations with strong contrasting effects on the two promoters, two which lie in the P_{TPCAD} −10 hexamer (238 and 209) are particularly interesting. Mutant 238, which also lies in the more start-site-proximal of the two pairs of −10 and −35 hexamer candidates for the *merR* promoter (Fig. 2, lighter-shaded boxes), strongly impairs unregulated P_R expression. In addition, one of the changes in double mutant 209 also lies within this candidate P_R −10 hexamer; here a nonconsensus A at what would be the −10 position becomes a consensus T, with a resulting 3.3-fold increase in unregulated P_R activity. Neither the change in 209 nor that in 238 affects any positions in the more start-site-distal −10 hexamer candidate. We conclude that the more start-site-proximal hexamer set of P_R (Fig. 2, lighter shading) is used in vivo. Thus, the −10 hexamers of P_{TPCAD} and P_R actually overlap by four

A

```
                -38    <------     ------>      -8
Tn21/501,Omr      TTGACTCCGTACATGAGTACGGAAGTAAGGT
pDU1358           ..............TG.............CT
Bacillus          ..T..C.T....TAAG.....TGGT.T.T.C
S. aureus         .....CGT....TATG....A.GGT.T.TAC
Single mutants    G.Δ...TT..C.....T.........SC...
Double mutants    ......TT..G.......C...T.......A
                        ^
                        C           T

Functional        TTKACYSYGTACWWWRGTACRKRRKTWAKSY
Consensus                     R                R
```

B

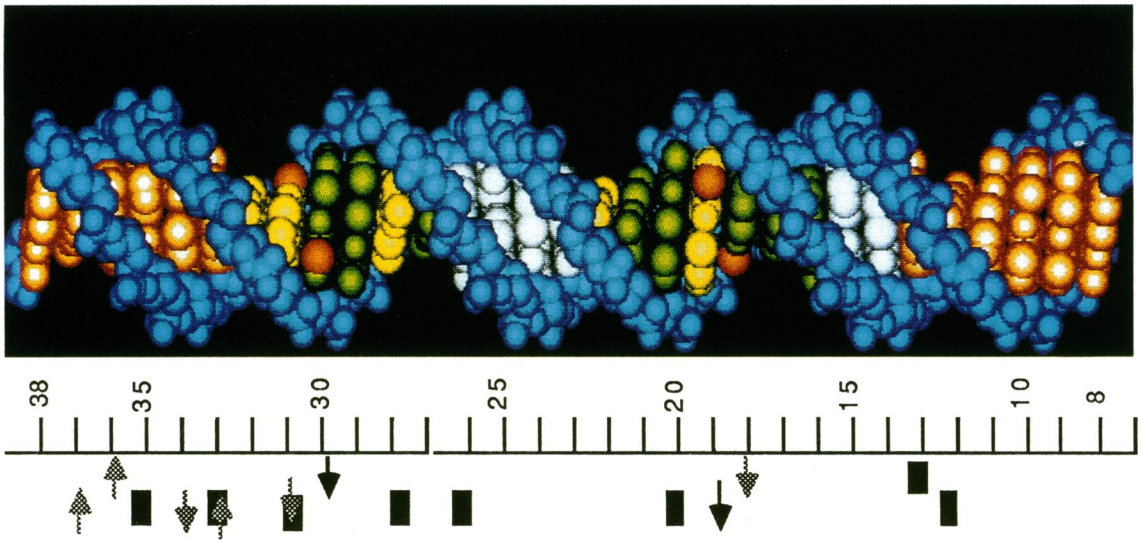

FIG. 3. (A) Consensus and function in *merOP*. Horizontal, diverging arrows indicate the palindromic sequence. A dot indicates no change from the Tn*21*/Tn*501* sequence. Underlining joins changes in double mutants. Variable bases in the functional consensus are designated according to International Union of Pure and Applied Chemistry nomenclature (K = G or T; R = G or A; S = G or C; W = T or A; Y = C or T). Sequence references are as follows: Tn*21* (2, 5), Tn*501* (5), Omr (from R831b [our unpublished observations]), *Bacillus* (17), *Staphylococcus aureus* (24), and mutants (this work). (B) Space-filling representation of the *merOP* region. Color code: darker blue, phosphate backbone; orange, −35 (left) and −10 (right); green, dyad bases in which no mutations were found; yellow, dyad bases in which mutations were found; red, guanine N-7s protected from dimethyl sulfate methylation in vivo by MerR (19). Numbering refers to position before start of the *merTPCAD* transcript. Note that the last base of the −35 hexamer overlaps with the first base in the left arm of the palindrome. Symbols below the number line indicate base reactivities from in vivo footprinting of wild-type Tn*21* (20); the vertical position of the symbol indicates whether the reaction affects an upper-strand base or a lower-strand base. Arrows pointing down show methylation protection (black = complete; grey = partial). Arrows pointing up show methylation enhancement. Protections at −18, −19, −30, and −31 are due to MerR; protections and enhancements at −33, −34, −36, and −37 are due to RNA polymerase (19). Solid boxes indicate enhanced reactivity with $KMnO_4$ upon induction; all are Ts (including −12 and −13 in the open complex) except for G-31 and A-33. Color rendition of the *merOP* sequence was produced by the MAKEDNA program of ProModeler software, New England Biographics, Inc.

bases, rather than being separated by one base as had been assumed in earlier work (18, 37). While these lighter-shaded (Fig. 2) candidate hexamers are close to consensus (32) and have optimal distance (6 bp) from the *merR* mRNA start compared with 11 bp for the more distal candidate −10 hexamer (Fig. 2, vertically striped boxes), their interhexamer spacing is 15 bp. Interestingly, the P_R interhexamer spacing is shorter by 2 bp and the P_{TPCAD} interhexamer spacing is longer by 2 bp than the consensus 17-bp spacing for sigma-70 promoters (13).

The generation of an alternative −35 hexamer in P_{TPCAD} may explain the unregulated expression of mutants 201 and 211 and the double mutant 214, which contains both of the changes in 201 and 211 (Table 2). The change in the up-expression mutant, 201 (C-31T), results in a potential alternative −35 hexamer with the sequence TGTACA from nt −31 to −26 (Fig. 2). This alternative −35 hexamer lies 18 nt upstream from the sequence TACGCT, which could serve as a −10 recognition site. These candidate hexamers are both reasonably close to the sigma-70 consensus (32), and the 18-bp spacing is closer to the optimum of 17 bp. We would expect that mutant 201, in its unregulated state, would have a different start site farther to the 3′ side of where it starts when under MerR-Hg(II) regulation. In contrast, mutant 211 (G-32T) is no stronger than the wild type as an unregulated promoter (Table 2); it would provide two alternative −35 hexamers, one beginning at −32 (TCGTAC) and the other beginning at −33 (TTCGTA) lying 19 and 20 bp, respectively, from the alternative candidate −10 hexamer, TACGCT, noted above. Neither the sequence nor the spacing of these alternatives in 211 is closer to the ideal than the wild-type promoter. Interestingly, double mutant 214's unregulated expression of P_{TPCAD} is greater than that of the wild type but considerably less than that of mutant 201; in the unregulated state, 214 may alternate between various hexamer sets. An additional −35 hexamer is also possible in 201 (TTGTAC, from nt −32 to −27); this hexamer is 19 bp upstream from another alternative −10 hexamer, TACGCT (Fig. 2) and would not be expected to be a strong promoter. Measurement of mRNA start positions for all three mutants under regulated and nonregulated conditions will reveal whether these distinct hexamer sets are used.

Thus, with relation to the current *merOP* consensus sequence, this set of mutants strongly indicates that the inner dyad positions are more significant in repression and activation than the outer positions (contrast mutants 201, 211, 214, and 209 with mutants 208, 255, 213, and 244). In addition, positions −22 (our observations) and −27 (42) are especially implicated in activation, perhaps serving a fulcrum function in the MerR-mediated DNA distortion which results from Hg(II) treatment (9, 19). A similar significance of bases nearer the dyad center was found in mutants of the O_1 *tet* operator, although, for technical reasons, that study examined only one side of the dyad (61). Our observations also confirm the designation of the −10 (mutants 209, 241, 206, and 238) and −35 (mutants 217 and 205) regions of P_{TPCAD} and identify the RNA polymerase recognition hexamers used in vivo at P_R (mutants 209 and 238).

(ii) Consideration of the mutants in light of DNA footprinting observations. In addition to the insights available from sequence comparisons, there is now also considerable evidence from in vitro and in vivo footprinting concerning which bases play significant roles in this region. With respect to *merOP* dyad positions, recent analyses (9, 19, 38) have demonstrated that MerR protects the N-7 positions of Gs at −18 (top strand), −19 (bottom strand), −30 (top strand), and −31 (bottom strand) (Fig. 3B) from methylation. In vivo the protections at −19 and −30 are essentially absolute, while those at −18 and −31 are slightly weaker (19) (Fig. 3B). Thus, MerR's physical contacts are stronger at the inner positions of the dyad arms than at the outer positions; we found alterations at position −19 (mutant 244) and at position −31 (mutants 201 and 214). We also found mutations at positions not previously identified as significant by methylation. Mutant 213 does affect a GC base pair, and recent in vivo methylation footprinting demonstrates a small but definite enhancement in methylation of G-22 in the wild-type *merOP* (25a). With respect to the −35 hexamer, occupancy of P_{TPCAD} by RNA polymerase has been revealed by purine methylation protections and enhancements just upstream of the left dyad arm (positions −33, −34, −36, and −37) (19, 38); of these, only position −36 has been found to be a very strong down-expression mutation (ΔG in this work [mutant 205] and G→A in reference 46 [mutant pWR126]).

In vivo permanganate footprinting has revealed MerR-Hg(II)-dependent increases in reactivity of bases in the P_{TPCAD} −10 hexamer (T-12, T-13, i.e., the open complex), in the −35 hexamer (A-33 and T-35), in the dyad interruption (T-26), and in the left (T-28 and G-31) and right (T-20) dyad arms (19) (Fig. 3B). In the present study, we found mutations that affect T-12 (206 and 241), T-28 (208 and 255), G-31 (201, 214, and 306), and T-20 (255). Note that the frequently mutated left dyad arm position, G-31, both is protected from methylation and becomes reactive with $KMnO_4$ upon induction. Its symmetrical counterpart in the right dyad arm, G-18 (the start position for *merR* mRNA transcription), although protected from methylation by MerR, was not found to be altered among this group of mutants and exhibits no inducible reactivity to $KMnO_4$ in the wild-type operon (19).

Thus, the observations reported here refine the biochemical determinations of the RNA polymerase binding positions; of the MerR contact positions −19, −20, −28, and −31; and of the location of the P_{TPCAD} open complex. Our data and those of Parkhill and Brown (42) also extend the set of significant dyad positions beyond those initially identified by footprinting to include −22 and −27; more recent in vivo methylation data do reveal slight methylation hypersensitivity at both positions (25a). Since we did not obtain any mutants in the four-base central dyad interruption (−23 to −26), our data do not reveal whether sequence is important at the two positions, −26 (9, 19) and −25 (9, 25a), which are distorted by the Hg(II)-MerR complex during induction. Further directed mutagenesis will assess the role of these positions in P_{TPCAD} expression.

In summary, this collection of mutants has demonstrated that a given base change may have distinct and even opposite effects on MerR's varied activities in this intimately overlapped regulatory region, established the RNA polymerase recognition sites used in vivo at the P_R promoter, confirmed the importance of certain bases identified as significant in footprinting studies, and extended the set of known functionally significant positions in *merOP* beyond those detected by dimethyl sulfate or $KMnO_4$ footprinting.

ACKNOWLEDGMENTS

We appreciate thoughtful discussions with Andreas Heltzel, Ike Lee, Wilma Ross, and Janet Westpheling and critical comments from the editor and two anonymous reviewers. We are grateful to Paul Totis for sequencing and for help with the fragment retardation assays.

This research was supported in part by NIH grant GM28211 to A.O.S.

REFERENCES

1. **Auble, D. T., T. L. Allen, and P. L. deHaseth.** 1986. Promoter recognition by *Escherichia coli* RNA polymerase: effect of substitutions in the spacer DNA separating the −10 and −35 regions. J. Biol. Chem. **261:**11202–11206.
2. **Barrineau, P., P. Gilbert, W. J. Jackson, C. S. Jones, A. O. Summers, and S. Wisdom.** 1984. The DNA sequence of the mercury resistance operon of the IncFII plasmid NR1. J. Mol. Appl. Genet. **2:**601–619.
3. **Bertrand, K. P., K. Postle, L. V. Wary, and W. S. Reznikoff.** 1983. Overlapped divergent promoters control expression of Tn*10* tetracycline resistance. Gene **23:**149–156.
4. **Brennan, R. G., S. L. Roderick, Y. Takeda, and B. W. Mathews.** 1990. Protein-DNA conformational changes in the crystal structure of a lambda Cro-operator complex. Proc. Natl. Acad. Sci. USA **87:**8165–8169.
5. **Brown, N., T. K. Misra, J. N. Winnie, M. Seiff, and S. Silver.** 1986. The nucleotide sequence of the mercuric resistance operons of plasmid R100 and transposon Tn*501*: further evidence for *mer* genes which enhance the activity of the mercuric detoxification system. Mol. Gen. Genet. **202:**143–151.
6. **Derbyshire, K., J. J. Salvo, and N. D. F. Grindley.** 1986. A simple and efficient procedure for saturation mutagenesis using mixed oligodeoxynucleotides. Gene **46:**145–152.
7. **de Vleig, J., H. J. C. Berendsen, and W. F. van Gunsteren.** 1989. An NMR-based molecular dynamics simulation of the interaction of the *lac* repressor headpiece and its operator in aqueous solution. Proteins Struct. Funct. Genet. **6:**104–127.
8. **Foster, T. J., H. Nakahara, A. A. Weiss, and S. Silver.** 1979. Transposon *A*-generated mutations in the mercuric resistance genes of plasmid R100-1. J. Bacteriol. **140:**167–181.
9. **Frantz, B., and T. V. O'Halloran.** 1990. DNA distortion accompanies transcriptional activation of the metal-responsive gene-regulatory protein MerR. Biochemistry **29:**4747–4751.
10. **Garner, M. M., and A. Revzin.** 1981. A gel electrophoresis method for quantifying the binding of proteins to specific DNA regions: application to components of the *Escherichia coli* lactose regulatory system. Nucleic Acids Res. **9:**3047–3060.
11. **Gaston, K., A. Bell, A. Kolb, H. Buc, and S. Busby.** 1990. Stringent spacing requirements for transcription activation by CRP. Cell **62:**733–743.
12. **Griffin, H. G., T. J. Foster, S. Silver, and T. K. Misra.** 1987. Cloning and DNA sequence of the mercuric and organomercurial-resistance determinants of plasmid pDU1358. Proc. Natl. Acad. Sci. USA **84:**3112–3116.
13. **Harley, C. B., and R. P. Reynolds.** 1987. Analysis of *E. coli* promoter sequences. Nucleic Acids Res. **15:**2343–2361.
14. **Harrison, S. C., and A. K. Aggarwal.** 1990. DNA recognition by proteins with the helix-turn-helix motif. Annu. Rev. Biochem. **59:**933–969.
15. **Hawley, D. K., and W. R. McClure.** 1983. Compilation and analysis of promoter DNA sequences. Nucleic Acids Res. **11:**2237–2255.
16. **Helmann, J. D., B. T. Ballard, and C. T. Walsh.** 1990. The MerR regulatory protein binds mercuric ion as a tri-coordinate, metal-bridged dimer. Science **247:**946–948.
17. **Helmann, J. D., Y. Wang, I. Mahler, and C. T. Walsh.** 1989. Homologous metalloregulatory proteins from both gram-positive and gram-negative bacteria control transcription of mercury resistance operons. J. Bacteriol. **171:**222–229.
18. **Heltzel, A., D. Gambill, W. J. Jackson, P. A. Totis, and A. O. Summers.** 1987. Overexpression and DNA-binding properties of the *mer*-encoded regulatory protein from plasmid NR1 (Tn*21*). J. Bacteriol. **169:**3379–3384.
19. **Heltzel, A., I. E. Lee, P. A. Totis, and A. O. Summers.** 1990. Activator-dependent preinduction binding of sigma-70 RNA polymerase at the metal-regulated *mer* promoter. Biochemistry **29:**9572–9584.
20. **Hendrickson, W., and R. Schleif.** 1985. A dimer of AraC protein contacts three adjacent major groove regions of the *ara*I DNA site. Proc. Natl. Acad. Sci. USA **82:**3129–3133.
21. **Hillen, W., and A. Wissman.** 1988. Tet repressor-*tet* operator interaction, p. 143–162. *In* W. Saenger and U. Heineman (ed.), Protein-nucleic acid interactions. The Macmillan Press Ltd., London.
22. **Inouye, S., and M. Inouye.** 1990. OmpR effects activation by enhancing binding of RNA polymerase to weak promoters. Cell **62:**530–539.
23. **Kammerer, W., U. Deuschle, R. Gentz, and H. Bujard.** 1986. Functional dissection of *Escherichia coli* promoters: information in the transcribed region is involved in late steps of the overall process. EMBO J. **5:**2995–3000.
24. **Laddaga, R. A., L. Chu, T. K. Misra, and S. Silver.** 1987. Nucleotide sequence and expression of the mercurial-resistance operon from Staphylococcus aureus plasmid pI258. Proc. Natl. Acad. Sci. USA **84:**5106–5110.
25. **Lathe, R., M. P. Kienny, S. Skory, and J. P. Lecocq.** 1984. Linker tailing: unphosphorylated linker oligonucleotides for joining DNA termini. DNA **3:**173–182.

25a. **Lee, I., and V. Livrelli.** Unpublished data.

26. **Lund, P. A., and N. L. Brown.** 1989. Regulation of transcription from the *mer* and *merR* promoters in the transposon Tn*501*. J. Mol. Biol. **205:**343–353.
27. **Lund, P. A., S. J. Ford, and N. L. Brown.** 1986. Regulation of expression of Tn*501 mer* genes. J. Gen. Microbiol. **132:**465–480.
28. **Mahler, I., H. S. Levinson, Y. Wang, and H. O. Halvorson.** 1986. Cadmium- and mercury-resistant *Bacillus* strains from a salt marsh and from Boston Harbor. Appl. Environ. Microbiol. **52:**1293–1298.
29. **McClure, W. R.** 1985. Mechanism and control of transcription initiation in prokaryotes. Annu. Rev. Biochem. **54:**171–204.
30. **Miller, J. H.** 1972. Experiments in molecular genetics. Cold Spring Harbor Laboratory, Cold Spring Harbor, N.Y.
31. **Misra, T. K., N. L. Brown, D. C. Fritzinger, R. D. Pridmore, W. M. Barnes, and S. Silver.** 1984. The mercuric ion resistance operons of plasmid R100 and transposon Tn*501*: the beginning of the operon including the regulatory region and the first two structural genes. Proc. Natl. Acad. Sci. USA **81:**5975–5979.
32. **Moyle, H., C. Waldburger, and M. M. Susskind.** 1991. Hierarchies of base pair preferences in the P22 *ant* promoter. J. Bacteriol. **173:**1944–1950.
33. **Mukhopadhyay, D., H. Yu, G. Nucifora, and T. K. Misra.** 1991. Purification and functional characterization of MerD. J. Biol. Chem. **266:**18538–18542.
34. **Ni'Bhriain, N. N., S. Silver, and T. J. Foster.** 1983. Tn*5* insertion mutations in the mercuric ion resistance genes derived from plasmid R100. J. Bacteriol. **155:**690–713.
35. **Oakley, M. G., and P. B. Dervan.** 1990. Structural motif of the GCN4 DNA binding domain characterized by affinity cleaving. Science **248:**847–850.
36. **Ogata, R., and W. Gilbert.** 1979. DNA binding site of *lac* repressor probed by dimethylsulfate methylation of the *lac* operator. J. Mol. Biol. **132:**709–728.
37. **O'Halloran, T., and C. T. Walsh.** 1987. Metalloregulatory DNA-binding protein encoded by the *merR* gene: isolation and characterization. Science **235:**211–214.
38. **O'Halloran, T. V., B. Frantz, M. K. Shin, D. M. Ralston, and J. G. Wright.** 1989. The MerR heavy metal receptor mediates positive activation in a topologically novel transcription complex. Cell **56:**119–129.
39. **Ohlendorf, D. H., W. F. Anderson, R. G. Fisher, Y. Takeda, and B. Matthews.** 1982. The molecular basis of DNA-protein recognition inferred from the structure of the *cro* repressor. Nature (London) **298:**718–723.
40. **Oliphant, A. R., C. J. Brandl, and K. Struhl.** 1989. Defining the sequence specificity of DNA-binding proteins by selecting binding sites from random-sequence oligonucleotides: analysis of yeast GCN4 protein. Mol. Cell. Biol. **9:**2944–2949.
41. **Pabo, C. O., A. K. Aggarwal, S. R. Jordan, L. J. Beamer, U. R. Obeysekare, and S. C. Harrison.** 1990. Conserved residues make similar contacts in two repressor-operator complexes. Science **247:**1210–1213.
42. **Parkhill, J., and N. L. Brown.** 1990. Site-specific insertion and deletion mutants in the *mer* promoter-operator region of Tn*501*: the nineteen base-pair spacer is essential for normal induction of the promoter by *merR*. Nucleic Acids Res. **18:**5157–5162.

43. **Poteete, A. R., and M. Ptashne.** 1982. Control of transcription by the bacteriophage P22 repressor. J. Mol. Biol. **157:**21–48.
44. **Ralston, D. M., and T. V. O'Halloran.** 1990. Ultrasensitivity and heavy-metal selectivity of the allosterically modulated MerR transcription complex. Proc. Natl. Acad. Sci. USA **87:**3846–3850.
45. **Risse, G., K. Jooss, M. Neuberg, H.-J. Bruller, and R. Muller.** 1989. Asymmetrical recognition of the palindromic AP1 binding site (TRE) by Fos protein complexes. EMBO J. **8:**3825–3832.
46. **Ross, W. E., S.-J. Park, and A. O. Summers.** 1989. Genetic analysis of transcriptional activation and repression in the Tn*21* *mer* operon. J. Bacteriol. **171:**4009–4018.
47. **Sanger, F., S. Nicklen, and A. R. Coulson.** 1977. DNA sequencing with chain-terminating inhibitors. Proc. Natl. Acad. Sci. USA **74:**5463–5467.
48. **Sarai, A., and Y. Takeda.** 1989. Lambda repressor recognizes the approximately 2-fold symmetric half-operator sequences asymmetrically. Proc. Natl. Acad. Sci. USA **86:**6513–6517.
49. **Sasmor, H. M., and J. L. Betz.** 1990. Symmetric *lac* operator derivatives: effects of half-operator sequence and spacing on repressor affinity. Gene **89:**1–9.
50. **Schevitz, R. W., Z. Otwinoski, A. Joachimiak, C. L. Lawson, and P. B. Singler.** 1985. The three dimensional structure of the *trp* repressor. Nature (London) **317:**782–786.
51. **Schneider, K., and C. F. Beck.** 1986. Promoter-probe vectors for the analysis of divergently arranged promoters. Gene **42:**37–48.
52. **Sellers, J. W., A. C. Vincent, and K. Struhl.** 1990. Mutations that define the optimal half-site for binding yeast GCN4 activator protein and identify an ATF/CREB-like repressor that recognizes similar DNA sites. Mol. Cell. Biol. **10:**5077–5086.
53. **Shewchuk, L. M., J. D. Helmann, W. Ross, S. J. Park, A. O. Summers, and C. T. Walsh.** 1989. Transcriptional switching by the MerR protein: activation and repression mutants implicate distinct DNA and mercury(II) binding domains. Biochemistry **28:**2340–2344.
54. **Shewchuk, L. M., K. Ivanetich, P. Prapunwattana, D. Santi, and C. T. Walsh.** Submitted for publication.
55. **Shewchuk, L. M., G. L. Verdine, and C. T. Walsh.** 1989. Transcriptional switching by the metalloregulatory MerR protein: initial characterization of DNA and mercury(II) binding activities. Biochemistry **28:**2331–2339.
56. **Staacke, D., B. Walter, B. Kisters-Woike, B. Wilcken-Bergmann, and B. Muller-Hill.** 1990. How Trp repressor binds to its operator. EMBO J. **9:**1963–1997.
57. **Summers, A. O.** 1986. Organization, expression, and evolution of the genes for mercury resistance. Annu. Rev. Microbiol. **40:**607–634.
58. **Takeda, Y., A. Sarai, and V. Rivera.** 1989. Analysis of sequence-specific interactions between Cro repressor and operator DNA by systematic base substitution experiments. Proc. Natl. Acad. Sci. USA **86:**439–443.

58a. **Totis, P.** Unpublished data.

59. **von Hippel, P. H., D. G. Bear, W. D. Morgan, and J. A. McSwiggen.** 1984. Protein-nucleic acid interactions in transcription: a molecular analysis. Annu. Rev. Biochem. **53:**389–446.
60. **von Hippel, P. H., and O. G. Berg.** 1989. DNA-protein interactions in the regulation of gene expression, p. 1–18. *In* W. Saenger, and U. Heineman (ed.), Protein-nucleic acid interactions. The Macmillan Press Ltd., London.
61. **Wissman, A., I. Meier, and W. Hillen.** 1988. Saturation mutagenesis of the Tn10-encoded *tet* operator O1: identification of base pairs involved in Tet repressor recognition. J. Mol. Biol. **202:**397–406.
62. **Wright, J. G., H.-T. Tsang, J. E. Penner-Hahn, and T. V. O'Halloran.** 1990. Coordination chemistry of the Hg-MerR metalloregulatory protein: evidence for a novel tridentate Hg-cysteine receptor site. J. Am. Chem. Soc. **112:**2434–2436.
63. **Yanisch-Perron, C., J. Vieira, and J. Messing.** 1985. Improved M13 phage cloning vectors and host strains: nucleotide sequences of the M13mp18 and pUC19 vectors. Gene **33:**103–119.